International Research Journal of Engineering and Technology (IRJET) e-ISSN: 2395-0056
Volume: 06 Issue: 03 | Mar 2019 www.irjet.net p-ISSN: 2395-0072

Flood Susceptibility Assessment through GIS-Based Multi-Criteria Approach and Analytical Hierarchy Process (AHP) in a River Basin in Central Greece

Lappas I.[1], Kallioras A.[2]

[1]Dr. Hydrogeologist, Special Secretariat for Water, Department of Protection and Management of Aquatic Environment, Division of Surface and Ground Waters, Amaliados 17 Str., Ambelokipi-Athens, P.C. 11523.
[2]Assistant Professor, National and Technical University of Athens, School of Mining and Metallurgical Engineering, Laboratory of Engineering Geology and Hydrogeology, Heroon Polytechniou 9 Str., Zografou-Athens, P.C. 15780.

Abstract - *Floods are considered to be one of the most cost effective natural hazards worldwide causing extended infrastructure damages devastating the affected area (properties, activities and environment) and relatively high death toll. This paper aimed at identifying the flood prone areas according to the study area's most triggering flood factors introducing multi-criteria indices and analysis. The multi-parametric approach was chosen to detect the area's most susceptible to floods within the Atalanti drainage basin in Central Greece as flood susceptibility mapping can be regarded essential in flood risk management. This method firstly used the flood factors assigned with the original weights and rankings (Ranking method) which resulted in a corresponding flood map and afterwards the use of pairwise comparison of Analytical Hierarchy Process (AHP) recalculated the factors' weights (relative impact weight based on priority) resulting in revised flood mapping. The flood causative factors considered in this essay were the rainfall intensity, namely, the modified Fournier index (MFI) derived from the mean monthly rainfall of a long time series (1981-2014), the flow accumulation based on the flow direction, the river basin's slope (in degrees), the land use/land cover derived from the CORINE 2012, the geology of the regional area, the soil type, the distance from the drainage network, the topographic wetness index (TWI) and finally, the elevation, all combined to determine an overall flood susceptibility through the region's digital elevation model (DEM). All the above mentioned weighted and ranked factors were divided into nine (9) classes ranging from Exceptionally Low to Exceptionally High spatially mapped with the integration of Geographical Information System (GIS) superimposed one thematic map to another resulting in a flood susceptibility map. The analysis results were subsequently used for the flood susceptibility delineation of those areas that are likely to suffer from significant flooding. Based on that almost 16% of the total area was categorized as the highest flood potential zone mainly at the eastern plain part of the study area (lowlands), whereas low flood potential zone covered approximately 43% of the total area encompassing the northwestern and southwestern parts of the study region as expected (hilly and mountainous areas). The assessment and mapping of flood spatial variability within the catchment could be used to construct the appropriate infrastructures and apply those measures with the least flood hazard during extreme and intense rainfall events as an effective tool for mitigation design strategies in flood prone areas. Finally, the index-based method could help identifying those parameters to make the decision support analysis concerned with water management as a prior condition for sustainable development.*

Key Words: natural hazards, flood areas delineation, weighted overlay factors, flood management, decision support analysis, Atalanti drainage basin

1. INTRODUCTION

Floods have become one of the worst natural hazards that cause damages worldwide in urban and rural areas with impact on people, agriculture, livelihood and infrastructures (Chen et al., 2009; 2015; Fernandez et al., 2010). Flood risk is globally increasing due to the rainfall pattern variations, the increase in extreme events, the changes in land use (e.g., deforestation), the population growth, etc. Moreover, the abrupt urbanization without the appropriate and multi-disciplinary spatial planning has already led to the occupation of improper areas such as river banks and floodplains within the inundation regions (Tsakiris, 2014). Thus, it is highly essential to be able to determine the flood susceptible areas for rational planning and flood management strategies. A detailed analysis of different criteria needs to be taken into account for a proper, more or less, decision analysis. For this purpose, Geographical Information Systems (GIS) offer the appropriate techniques to analyze the issue's numerous variables allowing the decision makers to identify a set of criteria for alternative plans and solutions that should apply protection and corrective measures (prioritization) to mitigate in a long term base the floods' disastrous effects within a basin (Domakinis et al., 2014; Jeb et al., 2008; Kourgialas et al., 2011). Obviously, mitigation practices can only be successful when thorough and deep knowledge is obtained as far as the magnitude of hazardous events and people awareness are concerned. A GIS-based multi-criteria approach in assessing the flood susceptible areas, through each parameter weight assignment, offers very satisfactory results in drainage basins with a priori well-known geomorphological and hydrological

parameters (Malczewski, 1999). Therefore, the aim of the presented study is to estimate the flood susceptible areas based on the flood factors identifying the most contributing ones.

This study, suitable for preliminary flood assessment, used the most appropriate heterogeneous geospatial criteria (index method integrated in a GIS environment) covering a wide range of the geo-environment, such as, topography, geomorphology, geology, hydrology and climate and applied a Multi-Criteria Analysis (MCA) to produce easily and rapidly at the end a flood susceptibility map divided into seven classes using semi-quantitative approaches such as ranking method and pairwise comparison (Analytical Hierarchy Process-AHP) as well to derive the priorities of the criteria in terms of their importance (Meyer et al., 2009a,b; Papaioannou et al., 2015; Sanders et al., 2000). The produced flood susceptibility map was finally compared taking into consideration the observed-historical floods at the regional area (Diakakis, 2017).

2. MATERIALS AND METHODS

2.1 Location Area

The Atalanti river basin belongs to the administrative Prefecture of Fthiotida (municipality of Lokri), in Central Greece, between $21^0 44'$-$24^0 39$ longitudes and $37^0 45$-$39^0 29'$ latitudes covering an area of approximately 250 km^2 (Fig -1). Generally speaking, the river basin has flat relief observed in lowlands with gentle slopes up to 20^0 and steeper one in highlands with slopes over 30^0 up to 55^0. The study area is washed by the sea at the East surrounded by hilly and mountain ranges (Lappas, 2018). Also, the catchment's altitude ranges between sea level and 1073 m (a.s.l.) crossed by dense, well developed, diverged and dendritic drainage network discharging into the East, in Aegean sea. Moreover, within Atalanti watershed, there are intermittent streams only, namely, Alargino, Karagkiozis (4th order by Strahler) and Ag. Ioannis (3rd order by Strahler) which flow only during winter and spring and form typical V-shape rejuvenated valleys as a result of the intensively active tectonics. Finally, the regional area is characterized by mild wet winters and hot, dry summers (typical Mediterranean climate with Csa type by Köppen) with the mean annual precipitation and the air temperature equals to 710.1 mm and 16.8^0C respectively (Lappas, 2018).

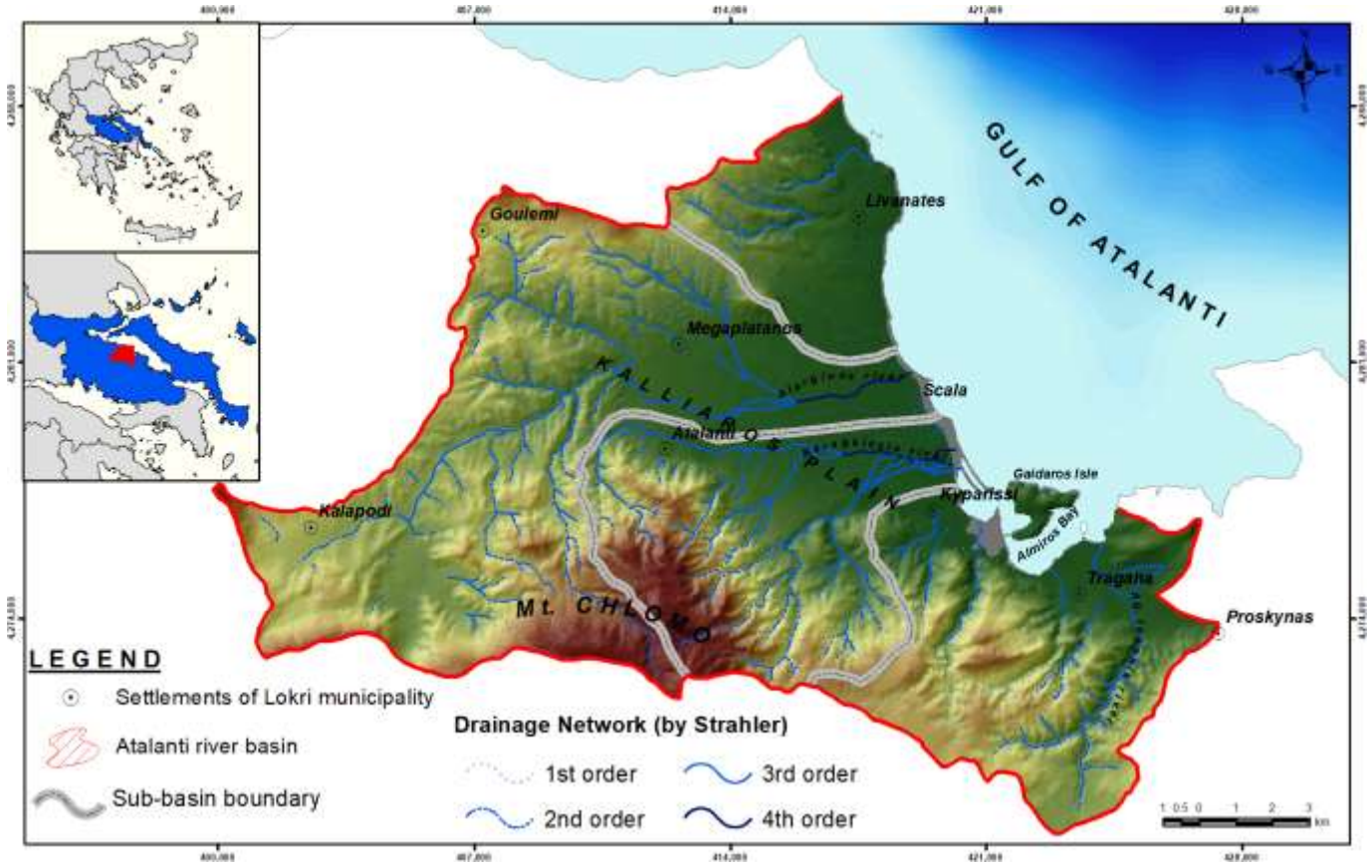

Fig -1: Site location of the Atalanti river basin with contributing drainage network

2.2 Data Sets

The geo-referenced in National Grid coordinating system (GGRS 87) and digitized topographic maps (20m interval) in scale 1:50,000 showing the drainage network of the Atalanti river basin were obtained from the Hellenic Military Geographical Service (HMGS). Based on those maps the digital elevation model (DEM of 25 m grid cell resolution) was derived, the sub-basins boundaries were also determined and several calculations were finally made as far as the area, the perimeter, the basin's slope, the flow direction and accumulation, the main flow length of each river tributary and the concentration time is concerned. Moreover, the digitized geological maps in scale 1:50.000 were obtained from the Institute of Geology and Mineral Exploration (IGME) to geologically characterize the formations concerning their contribution to floods. Furthermore, monthly rainfall dataset for a large time period (1981-2014) from 17 meteorological stations covering the regional area were obtained from the Hellenic National Meteorological Service (HNMS) and the Ministry of Environment and Energy. This kind of data helped to design the rainfall distribution maps for each month (mean value) and eventually the rainfall intensity was mapped. Also, through CORINE Land Cover (2012), the study area's land use was identified and categorized according to flood susceptibility. Taking into account the soil type map within the study area, produced and published by the Agriculture University of Athens, each soil was classified and ranked according to its texture and vulnerability to flood event. All the aforementioned base and derived thematic spatial maps were pre-processed, analyzed and integrated together in a GIS environment transformed into a grid spatial database and classified into seven classes on the basis of theirs effect on flooding to display spatial information so as to finally identify the flood prone areas, namely, a multi-layered map of similar flood potential within the catchment. At the end, historical flood events were used to validate the results.

2.3 Methodology Analysis

A semi-quantitative index-based model was developed in a GIS geo-processing environment aiming to define flood susceptible areas through the criterion weighting for expressing each criterion's importance to other criteria. The Multi-Criteria Analysis (MCA) process was performed in order to determine the flood causative factors analyzing a series of alternatives with a view to ranking them from the most preferable to the least preferable (De Brito et al., 2016; 2018; Yahaya et al., 2010; Yalcin et al., 2004a,b). This was succeeded by applying two methods, namely, the ranking method and the pairwise comparison one through Analytical Hierarchy Process (AHP) (Saaty, 1977; 1980; 1990) used for decision making and based on a quantitative assessment of the various factors being considered. Flood Susceptibility Index (FSI) consisted, as mentioned before, of nine variables-criteria, namely, the rainfall intensity (I), the flow accumulation (F), the basin's slope (in degrees) (S), the land use (U), the geology (G), the soil type (S_T), the distance from the drainage network (D), the topographic wetness index (TWI) and the elevation (E). The selection of these parameters was actually based on their relevance to flood occurences as documented in the literature (Bathrellos et al., 2016; Emmanouloudis et al., 2008; Karymbalis et al., 2012; Kazakis et al., 2015; Kourgialas et al., 2017; Patrikaki et al., 2018; Pradhan, 2010; Tsitroulis et al., 2016; Youssef et al., 2011). Each parameter was spatially visualized in a thematic map after having been processed in a GIS environment using a weighted overlay analysis and was categorized into seven classes from "Very Low" to "Very High". To classify the actual values into groups the Jenks natural breaks classification method in GIS was used as the best arrangement of values into different classes. Following the weights' calculation (Fig -2), the FSI was calculated using the following equation:

$$FSI = \sum_{i=1}^{n} w_i R_i$$

where,

R_i the rating of each variable/criterion
w_i the variable's weight assignement
n the number of variables/criteria

Ranking method

Each parameter was assigned a value in a scale between 1 and 10 (rating score) and the classes as well as the weights were defined using the grading method of natural breaks and the literature, respectively. Also, the qualitative parameters were classified based on previous studies. In ranking method, every criterion under consideration is ranked in the order of the decision expert's consultation, knowledge, experience and subjectiveness. To make the various criterion maps comparable, a standardization procedure of the raw data was required through weighted-linear scale transformation. The normalized rate was calculated based on the sum of the rates assigned on each parameter.

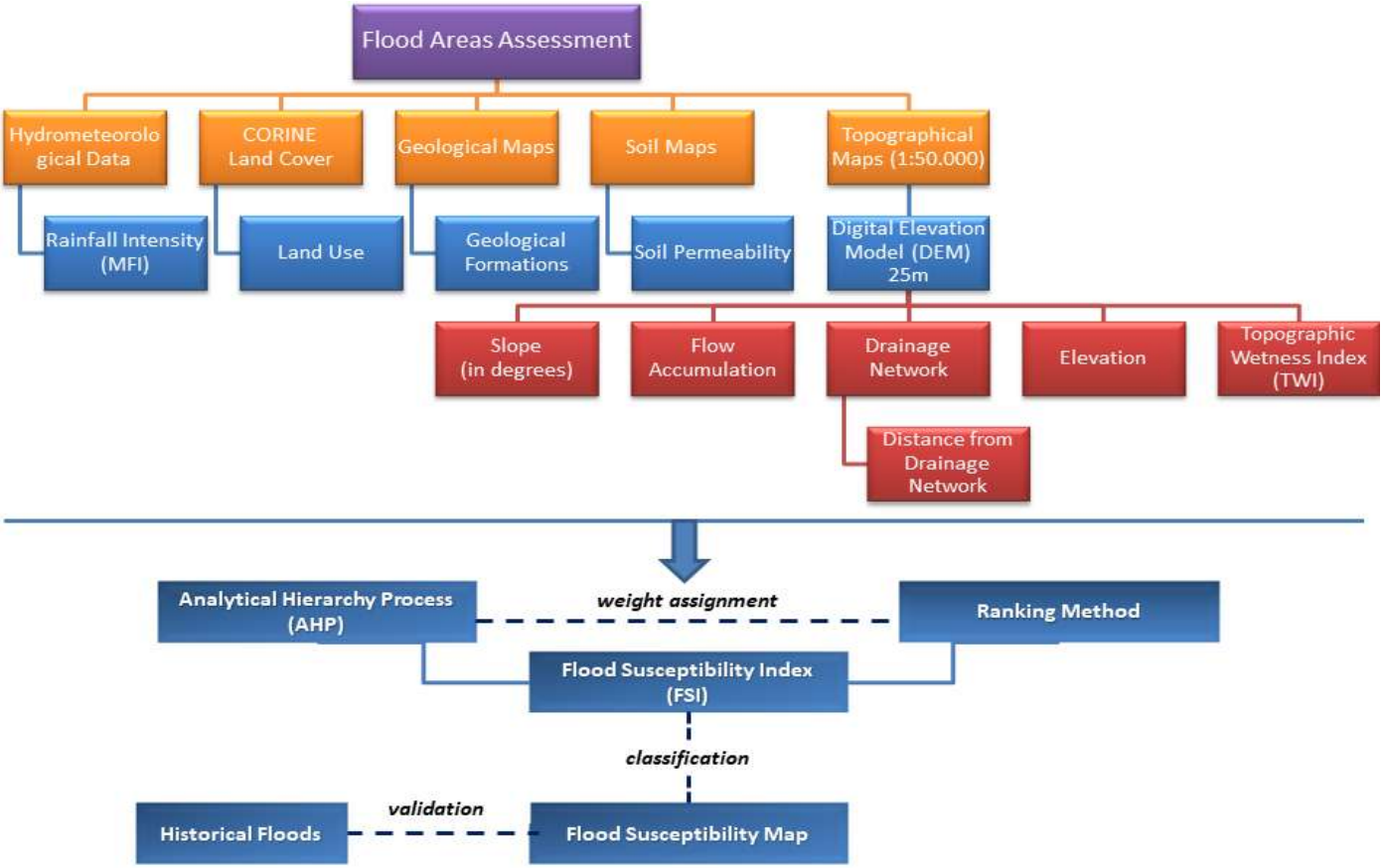

Fig -2: Methodology flowchart

Pairwise comparison method

The AHP method helps in detecting the flood susceptibility areas in the study area by identifying the most flood significant criteria based on the decision makers' preferences being capable of converting subjective assessments of relative importance into a linear set of weights (Kandilioti et al., 2012; Myronidis et al., 2009; Stefanidis et al., 2013). This approach was used for comparing each factor map and determining the factor weight values. Furthermore, the criterion pairwise comparison matrix (9×9) takes the pairwise comparisons as an input and produces the relative weighting factors allowing the comparison of two criteria at a time. The relative significance between the criteria is evaluated along the row from 1 to 9 indicating less important to much more important criteria, respectively whereas the reciprocal of the weight (from 1/2 to 1/9) is assigned to the corresponding column. Moreover, the final weightings for the parameters are the normalized values of the eigenvectors that is associated with the maximum eigenvalues of the reciprocal matrix. The Consistency Ratio measures how far a matrix is away from consistency. A Consistency Ratio (CR) indicates the probability that the matrix ratings were randomly generated and when CR is less than or equal to the threshold 0.1 (Table -1) signifies an acceptable reciprocal matrix, while ratio over 0.1 implies that the matrix should be revised indicating inconsistent judgments and is given by the equation:

$$CR = CI / RI$$

where,

CI the Consistency Index given by the equation:

$$CI = (\lambda_{max} - n) / (n - 1)$$

where,

λ_{max} the maximum eigenvalue (priority vector multiplied by each column total)
n the number of variables/criteria involved and
RI the Random Index (Table 1) for matrices which is based on the number of variables (n)

Table -1: Random Index (RI) used to CR computation

n (variables/criteria)	1	2	3	4	5	6	7	8	9	10
Random Index (RI)	0.00	0.00	0.58	0.90	1.12	1.24	1.32	1.41	1.45	1.49

3. RESULTS AND DISCUSSION

3.1 Variables/Criteria Selected

Rainfall Intensity (I)

Heavy rainfalls are one of the main flood-triggering causes. Both the local and regional rainfalls were integrated due to the limited size of the study area. In the present essay, monthly precipitation data (Chart -1) of 34 years (1981-2014) from 17 adjacent rain gauge stations collected from the Hellenic National Meteorological Service (HNMS) and the Ministry of Environment and Energy were used to calculate the rainfall intensity through the Modified Fournier Index (MFI) and interpolated to create a continuous raster rainfall map within and around the study area.

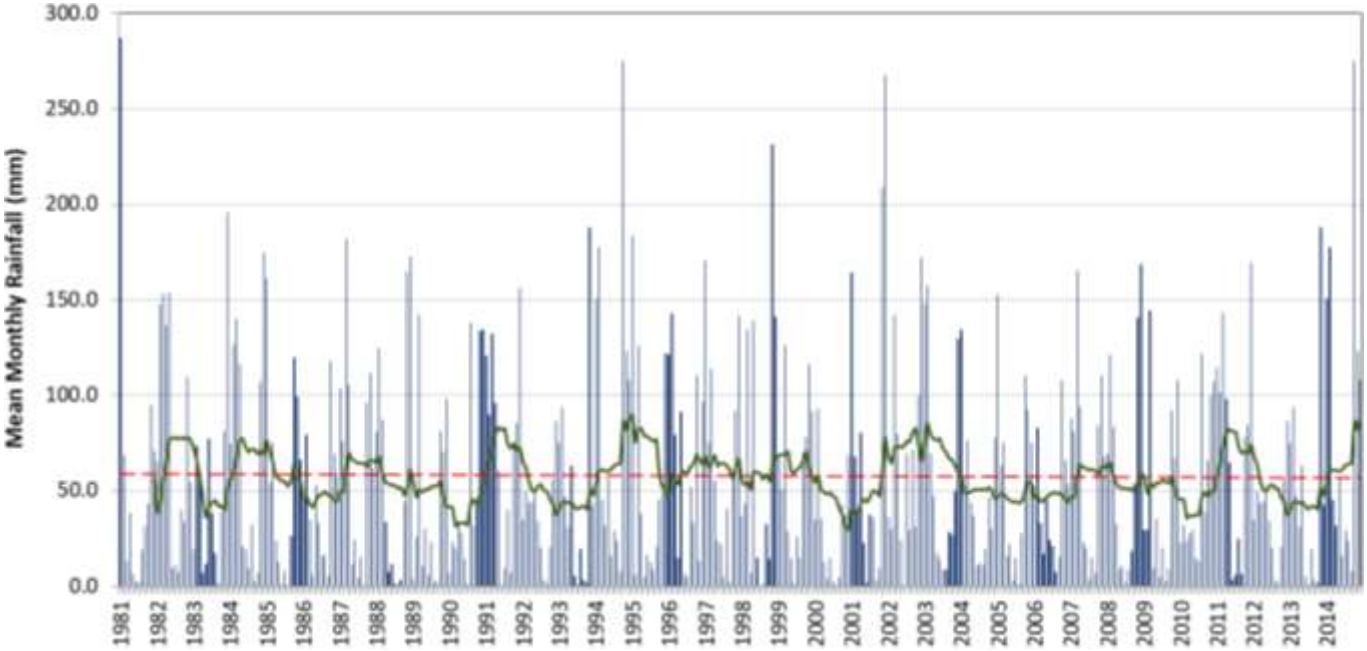

Chart -1: Mean monthly rainfall values in the study area. The red dashed line shows the average precipitation value of the time series (1981-2014) and the green solid one the 12-month moving average

The Modified Fournier Index-MFI (dimensionless) which is the sum of the average monthly rainfall intensity is given by the following equation:

$$MFI = \sum_{i=1}^{12} P_i^2 / P$$

where,

P_i the mean precipitation (mm) for each month
P the mean annual precipitation (mm)

The values of this parameter were classified into seven classes between MFI = 47.4 and MFI = 152. As illustrated in Fig -3 the higher values were located in the hilly and mountainous parts of the study area whereas the lower ones in the flat relief (Kalliaros plain), as expected.

Flow Accumulation (F)

The flow accumulation is the most important factor in deleaniting flood susceptibility areas. High values of accumulated flow indicated regions of concentrated flow and eventually prone to higher flood hazard. The flow accumulation values varied (Fig -4) with the highest ones occurring in the outflow (lowlands) of Alarginos and Karagkiozis tributaries whereas lower values occurring in streams in highlands.

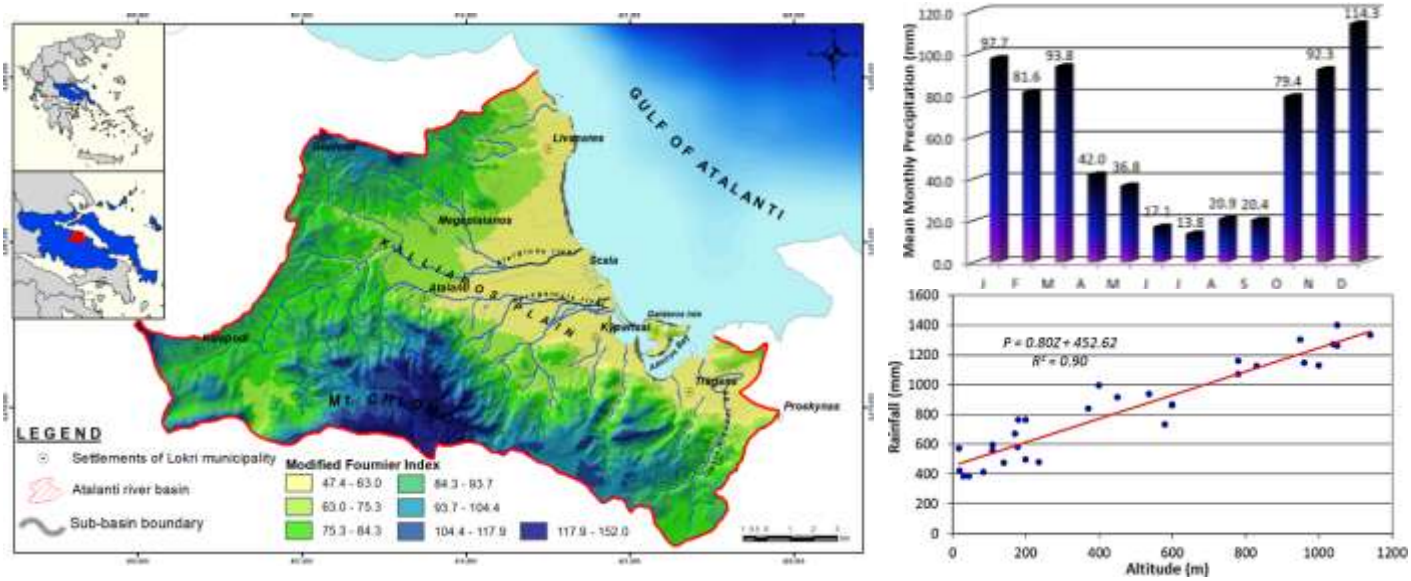

Fig -3: Rainfall intensity map (1981-2014) based on Modified Fournier Index-MFI. On the right, the mean monthly precipitation for the entire time period and the rain gradient equation for the regional area according to linear regression analysis

Slope (S)

The flash floods increase as the surface slope increases due to the augmentation of flow velocity affecting the surface runoff and causing flood areas across the lowlands. Steeper slopes are more susceptible to surface runoff since high slope gradients do not accumulate the surface water, while flat areas are vulnerable to flood occurrences. Geomorphologically, the slope varies with high slopes (30°-55°) in the mountainous areas, moderate to steep slopes (10°-30°) in the hilly areas and gentle to moderate slope (0°-10°) in the plain. The slope map (Fig -4) of the Atalanti basin was reclassified into seven (7) classes varing from 0–5 to >45% with a mean slope of 10.5° and standard deviation of 8.8°.

Land Use (U)

Land use affects infiltration rate with forest and vegetated areas favoring infiltration, while urban, residential and pasture areas aggregating the overland flow due to the impervious cover which reduces infiltration capacity and increases runoff showing high susceptibility to flooding. According to Corine Land Cover European programme (2012) the study area is covered by 13 discrete land use categories from which the highest percent is occupied by sclerophyllous vegetation (29.7%), another percent by non-irrigated arable land (20.5%), (16.6%) and complex cultivation patterns (11.7%), a relatively small percent by transitional woodland – shrub (9.7%) and land principally occupied by agriculture with significant areas of natural vegetation (6.9%) and finally, areas with mixed forest (2.3%), natural grasslands (1.4%) and discontinuous urban fabric (1.2%). In the Land Use map (Fig -4), seven (7) classes were identified, namely, urban/residential areas, forests, olive groves and vineyards, croplands, sclerophyllous vegetation, non-arable land and transitional lands.

Geology (G)

The regional area is consisted of metamorhic-ultrabasic rocks of Paleozoic age such as shales and schists, of ophiolithic rocks (diabases, peridotites, serpentines) and flysch and of formations from Triassic to Createaceous age (e.g. dolomites and limestones) with large-scale faulting zones (WNW and NNE directions), fractures, fissures and cracks. Post-alpine mostly unconsolidated sediments such as sandstones, conglomerates, marls and alluvial deposits of Tertiary (Neogene-Pleiocene) and Quaternary age (Maratos et al., 1965) cover the Kalliaros plain. Permeable and karstic formations favor groundwater infiltration, whereas impermeable ones, such as crystalline rocks, favor surface runoff. In the geological map the geological formations were considered and ranked based on the hydraulic conductivity. According to the geology, seven (7) classes were

considered with crystalline rocks being attributed the highest rate, marls the medium one and dolomites-limestones as well as the alluvial deposits with the lowest rate value because of their medium to high infiltration capacity (Fig -4).

Soil Type (S_T)

Soil type and texture are infiltration factors and eventually affect flood susceptibility. Surface runoff is likely to be more rapid and greater with clay soils than with sand ones. Most of impermeable soils consist of clay which make them prone to flooding, while soils consisted of sands are permeable and relatively easily infiltrated since they may absorb great amount of surface water. Generally speaking, the soil type is able to control the amount of water that can be infiltrated into the ground. The weighted soil map was prepared by assigning weights to each soil class (Fig -5). For the case study, several lithological units were identified based on infiltration capacity and were considered into the three broad categories, namely, highly infiltrated (lowest rate value), moderately infiltrated (medium rate value) and less infiltrated (highest rate value).

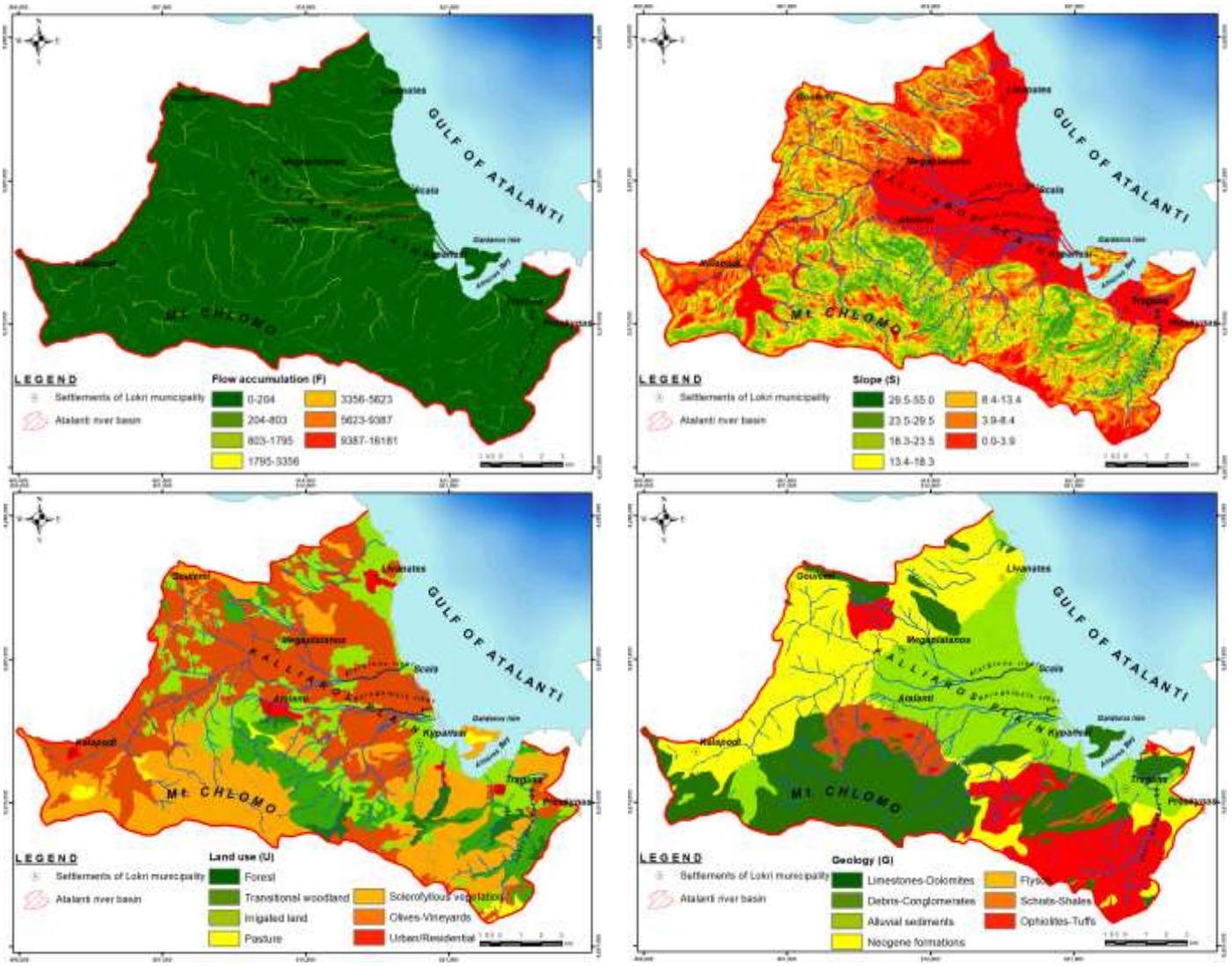

Fig -4: Thematic maps of flow accumulation, slope, land use and geology with classification

Distance from Drainage (D)

The distance from river network plays an important role in defining the flooding areas. The role of a river decreases as the distance from river banks increases. For the study area, it appears that areas near the river network (<50 m) are highly flood susceptible, while the effect of this parameter significantly decreases in distance >500 m. The most affected areas during floods are those near the river channels as a consequence of overflow. The drainage network was reclassified in seven classes and

areas with high distance from drainage were ranked with the lowest rate value while those with low drainage distance were ranked with the highest rate value, as illustrated in Fig -5.

Topographic Wetness Index (TWI)

The Topographic Wetness Index (TWI) was developed by Beven & Kirkby (1979) combining the upstream contributing area per unit and slope and is mostly used to quantify topographic control on hydrological processes and distribute the soil moisture in a given area (Fig -5). The TWI is given by the equation:

$$TWI = \ln(\alpha/\tan\beta)$$

where,

a the upslope contributing area (flow accumulation raster map for the corresponding DEM)
tanβ the slope angle (the slope raster map in degrees for the corresponding DEM)

High values represent drainage depressions (lowlands with low slope gradient) with wet ground while low ones represent crests and ridges (highlands with high slope gradient). The higher value of TWI the more susceptible areas to flooding.

Elevation (E)

Flat areas may flood quicker than areas in hills and mountains with steeper slopes as surface water flows from higher to lower altitude. Naturally, low elevation areas have been assigned the highest rating, as flood prone areas (Fig -5). Within the study area, the mountainous areas account only for 2.2% (>800 m) of the total area mainly at the Southern end of the basin (Mt. Chlomo). The semi-mountainous topographical zone accounts for 4.5% (600-800 m) while the flat areas account for 39.5% (0-200 m) mostly concerning the coastal areas. Also, the hilly and semi-hilly areas occupy almost 54% (200-600 m) of the basin.

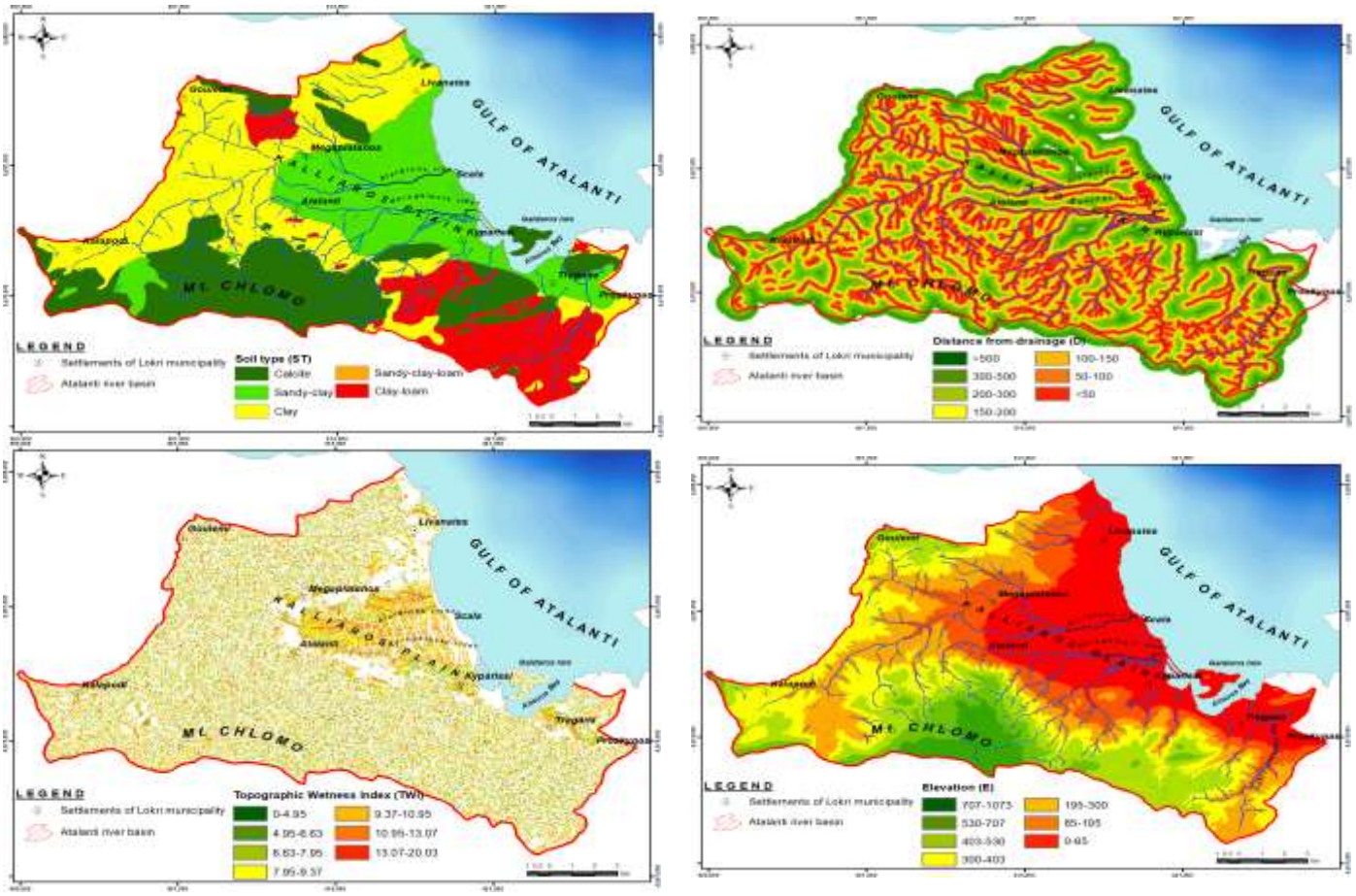

Fig -5: Thematic maps of soil type, distance from drainage network, topographic wetness index and elevation with classification

3.2 Flood Susceptibility Map Based on Ranking Method

According to Ranking method the rating score of each variable/criterion ranged from 1 to 10 indicating the classes from "Very Low" to "Very High", respectively. Then, each variable was assigned to a unique weight based on expert judgment, decision-maker's preference and scientific literature. The total weight was resulted by the sum up of the weight and ranking multiplication. After following the same procedure for all the aforementioned criteria, the gross weight of the total one is shown in Table -2. According to this technique, each factor is multiplied by its percent weight and the summation of all factors yields the final map of susceptible areas All the criteria used quantitative (numeric) parameters except for the factors "geology", "land use" and "soil type" (qualitative-descriptive form). In the case of the non-numeric factors, classification depends mainly on the influence of the factor on the recharging flood process. The ratios of factors according to their impacts on flood susceptibility were determined for the flow accumulation, the basin's slope, the land use, rainfall intensity, the geology, the soil type, the distance from the drainage network, the topographic wetness index and the elevation by 6.62%, 8.83%, 11.03%, 6.62%, 13.3%, 9.46%, 11.03%, 15.45%, 17.66, respectively. These criteria all combined based on their proportions were resulted in the flood susceptibility map shown in Fig -6. Since all factors do not have the same degree of influence on the hazardous areas, a weighting approach, in which a different weight is assigned to each factor, was applied. The elevation and the TWI as well were assigned with the highest weights followed by the geology, the soil type, the distance from drainage network and the land use. On the contrary, the flow accumulation, the rainfall intensity as well as the slope were assigned with the lowest weights. As illustrated in Fig -6 the classes "Moderate to High", "High" and "Very High" cover a surface of 62.25% or 153.54 km^2 of the total basin area which mainly belongs to the flat relief of the Atalanti river basin and to areas close to the outputs of the main rivers at the East, as expected. On the contrary, the other classes cover higher slope gradient areas which are far away from the high drainage density ones. Finally, as shown in Fig -6 the flooded areas (hatched region) based on historical records fall within the classes "High" and "Very High" validating the reliability of the applied methodology.

Table -2: Variables/criteria contributing to flood susceptibility based on Ranking method

Variables/Criteria	Range	Classes	Ranking-x_i	Weight-w_i	$w_i x_i$	Total Weight	Share (%)
Flow Accumulation (F)	0-204	Very Low	1.0	1.5	1.5	57.75	6.62
	204-803	Low	2.5		3.75		
	803-1795	Low to Moderate	4.0		6.0		
	1795-3356	Moderate	5.5		8.25		
	3356-5623	Moderate to High	7.0		10.5		
	5623-9387	High	8.5		12.75		
	9387-16181	Very High	10.0		15.0		
Slope (degrees) (S)	29.5-55.0	Very Low	1.0	2.0	2.0	77.0	8.83
	23.5-29.5	Low	2.5		5.0		
	18.3-23.5	Low to Moderate	4.0		8.0		
	13.4-18.3	Moderate	5.5		11.0		
	8.4-13.4	Moderate to High	7.0		14.0		
	3.9-8.4	High	8.5		17.0		
	0.0-3.9	Very High	10.0		20.0		
Land Use (U)	Forest	Very Low	1.0	2.5	2.5	96.25	11.03
	Transit. Woodland	Low	2.5		6.25		
	Irrigated land	Low to Moderate	4.0		10.0		
	Pasture	Moderate	5.5		13.75		
	Sclerofyl. Vegetat.	Moderate to High	7.0		17.5		
	Olives-Vineyards	High	8.5		21.25		
	Urban/Residential	Very High	10.0		25.0		
Rainfall Intensity-MFI (I)	47.4-63.0	Very Low	1.0	1.5	1.5	57.75	6.62
	63.0-75.3	Low	2.5		3.75		
	75.3-84.3	Low to Moderate	4.0		6.0		
	84.3-93.7	Moderate	5.5		8.25		
	93.7-104.4	Moderate to High	7.0		10.5		
	104.4-117.9	High	8.5		12.75		
	117.9-152.0	Very High	10.0		15.0		
Geology (G)	Limestones-Dolom.	Very Low	1.0	3.0	3.0	115.5	13.3
	Debris-Conglom.	Low	2.5		7.5		
	Alluvial sediments	Low to Moderate	4.0		12.0		
	Neogene formations	Moderate	5.5		16.5		

Variables/Criteria	Range	Classes	Ranking-x_i	Weight-w_i	$w_i x_i$	Total Weight	Share (%)
	Flysch	Moderate to High	7.0		21.0		
	Schists-Shales	High	8.5		25.5		
	Ophiolites-Tuffs	Very High	10.0		30.0		
Soil Type (S_T)	Calcite	Very Low	1.0	3.0	3.0	82.5	9.46
	-	Low	-		-		
	Sandy-clay	Low to Moderate	4.0		12.0		
	Clay	Moderate	5.5		16.5		
	Sandy-clay-loam	Moderate to High	7.0		21.0		
	-	High	-		-		
	Clay-loam	Very High	10.0		30.0		
Distance from Drainage (m) (D)	>500	Very Low	1.0	2.5	2.5	96.25	11.03
	300-500	Low	2.5		6.25		
	200-300	Low to Moderate	4.0		10.0		
	150-200	Moderate	5.5		13.75		
	100-150	Moderate to High	7.0		17.5		
	50-100	High	8.5		21.25		
	<50	Very High	10.0		25.0		
Topographic Wetness Index (TWI)	0-4.95	Very Low	1.0	3.5	3.5	134.75	15.45
	4.95-6.63	Low	2.5		8.75		
	6.63-7.95	Low to Moderate	4.0		14.0		
	7.95-9.37	Moderate	5.5		19.25		
	9.37-10.95	Moderate to High	7.0		24.5		
	10.95-13.07	High	8.5		29.75		
	13.07-20.03	Very High	10.0		35.0		
Elevation (m) (E)	707-1073	Very Low	1.0	4.0	4.0	154.0	17.66
	530-707	Low	2.5		10.0		
	403-530	Low to Moderate	4.0		16.0		
	300-403	Moderate	5.5		22.0		
	195-300	Moderate to High	7.0		28.0		
	85-195	High	8.5		34.0		
	0-85	Very High	10.0		40.0		
Total	-	-	-	-	-	**871.75**	**100.0**

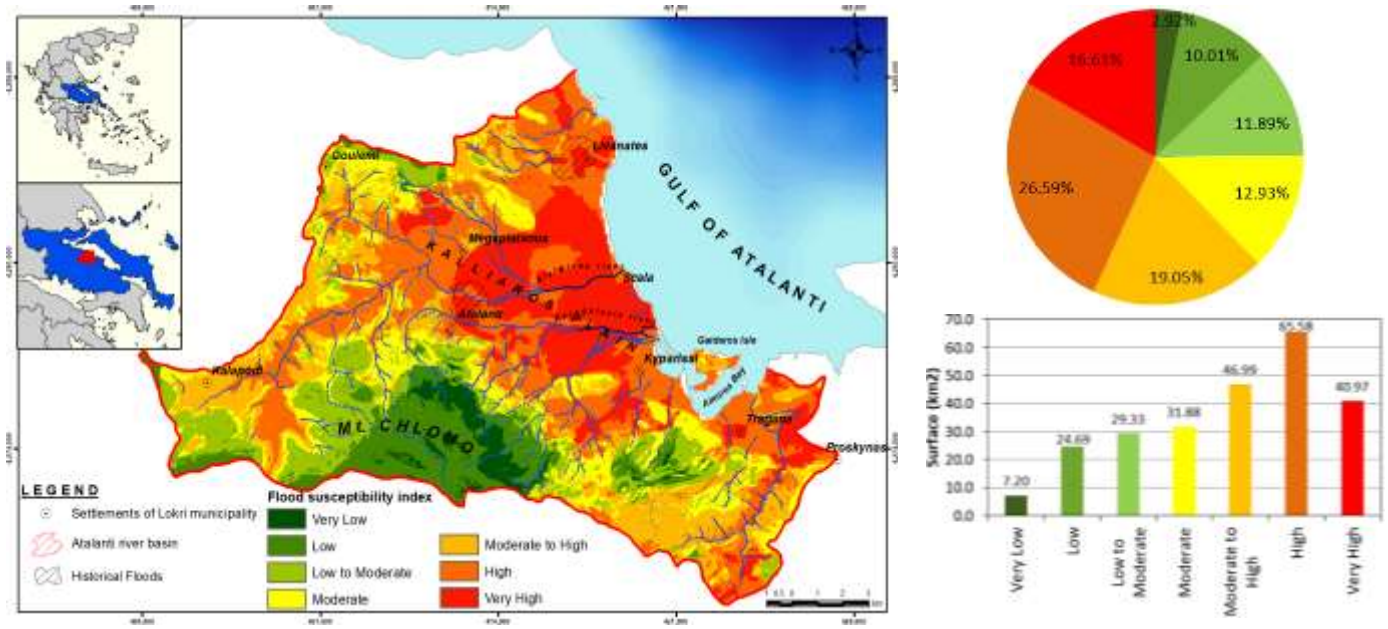

Fig -6: Flood susceptibility map based on Ranking method (left) and classes' surface distribution percentage (right)

3.3 Flood Susceptibility Map Based on AHP Method

Seven flood-prone categories ranging from "Very low" to "Very high" were identified using the natural breaks method. The main drawback of the AHP method is the subjectivity and the arbitrary, more or less, of experts' judgments of the weights' initial estimation with the higher weight value representing more priority than others. However, the pairwise comparison and the weights' normalization as well are important to reduce bias and uncertainty in the final result. As shown in Table -3, the factors "TWI", "elevation" and "distance from drainage" were proved to be the most significant ones contributing to flooding (24.4%, 19% and 18%, respectively) while the factors "geology", "soil type" and "flow accumulation" (3.4%, 4.3% and 4.3%, respectively) were finally considered as the lowest effects on flood susceptibility. Also, the consistency ratio was much below the threshold value of 0.1 (CR=0.058) which indicated consistent judgments, thus, the weights were acceptable. As illustrated in Fig.8, the classes "Moderate to High", "High" and "Very High" cover a surface of 53.15% or 130.85 km^2 of the total basin area where low slope gradient prevails (low elevation areas) and urbanization exists (population density). Moreover, the land use of the above classes (flooded areas) is mainly agricultural, non-arable and bare soil as well and is found nearby the river banks (drainage network) while at the southern part of the basin the flooding areas are rarely found meaning less sensitive to floods due to high terrain, high slope gradients and forested areas (Mt. Chlomo). Finally, as illustrated below (Fig -7) the flooded areas according to historical flood-events fall within the classes "High" and "Very High" verifying the successful application of the proposed methodology.

Table -3: Variables/criteria weights' assignment to flood susceptibility based on AHP method

Variables/Criteria	Topographic Wetness Index	Distance from Drainage	Elevation	Land Use	Rainfall Intensity	Slope	Geology	Soil Type	Flow Accumulation	Final Weight (by Eigen)
Topographic Wetness Index	**1**	2	2	3	3	4	7	5	2	***0.244***
Distance from Drainage	1/2	**1**	1	3	3	3	6	4	3	***0.180***
Elevation	1/2	1	**1**	3	3	3	6	4	5	***0.190***
Land Use	1/3	1/3	1/3	**1**	2	2	5	3	3	***0.107***
Rainfall Intensity	1/3	1/3	1/3	1/2	**1**	2	5	3	3	***0.094***
Slope	1/4	1/3	1/3	1/2	1/2	**1**	3	2	2	***0.065***
Geology	1/7	1/6	1/6	1/5	1/5	1/3	**1**	1	2	***0.034***
Soil Type	1/5	1/4	1/4	1/3	1/3	1/2	1	**1**	2	***0.043***
Flow Accumulation	1/2	1/3	1/5	1/3	1/3	1/2	1/2	1/2	**1**	***0.043***
Sum	**3.76**	**5.75**	**5.62**	**11.87**	**13.37**	**16.33**	**34.50**	**23.50**	**23.00**	***CR=0.058***

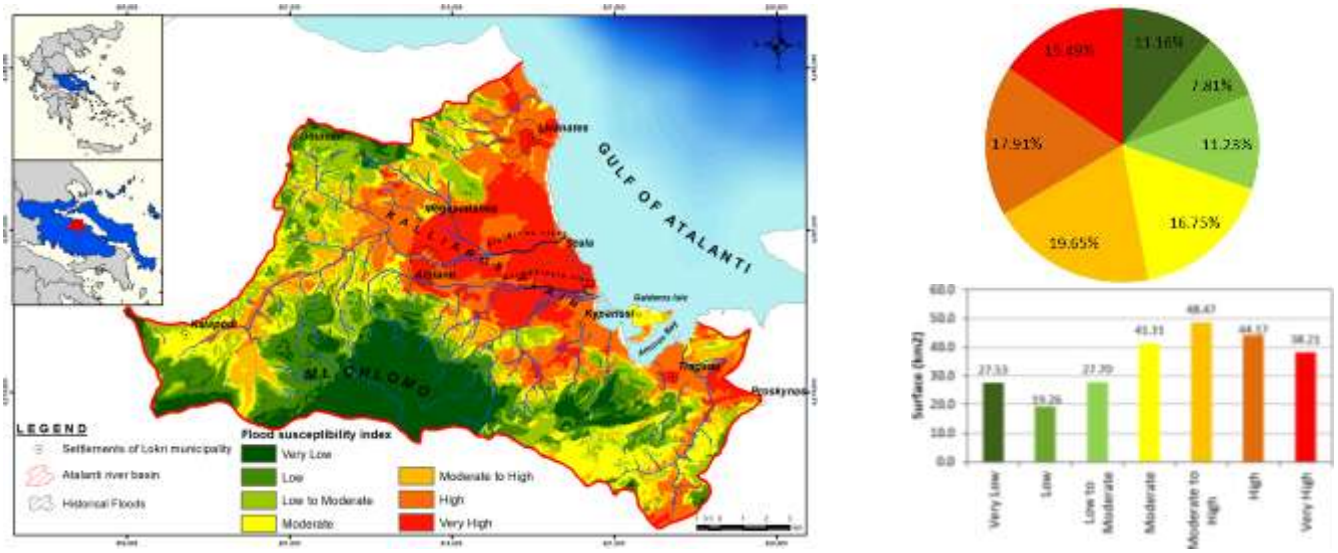

Fig -7: Flood susceptibility map based on AHP method (left) and classes' surface distribution percentage (right)

3.4 Methods' Comparison

As described, two multi-criteria vulnerability maps were created. The different results obtained from these two methods indicate the importance of the decision and policy makers to determine the weights and the appropriate method which suits the most. It is clearly obvious that the weighting of the different criteria significantly affects the results of the overall evaluation since the rating for each criterion may differ from scientist to scientist. As shown in Table -4 and Chart -2, the main differences were observed in two classes, namely, "Very Low" and "Very High". Specifically, the Ranking method had the lowest value in "Very Low" class and the highest one in "High" class while the AHP method had the lowest value in "Low" class and the highest one in "Moderate to High" class. Moreover, based on Ranking method the highest weight was assigned to "Elevation" criterion (17.7%) and the lowest one to "Rainfall Intensity" (6.6%). However, on AHP method the highest weight was assigned to "TWI" criterion (24.4%) and the lowest one to "Geology" (3.4%) whereas "Geology" criterion on Ranking method was ranked third in significance. Also, as illustrated below, in weight vs. criteria graph (Chart -2) the weight range was greater in AHP method (21%) than in Ranking method (11.1%) indicating abrupt and smooth susceptibility changes, respectively. In any case, both methods were proved to be greatly accurate since the recorded available flood events (historical observed floods) were classified within the highly susceptible areas showing also that the whole flat plain (Kalliaros) at the East is the most flood susceptible area.

Table -4: Results' comparison between Ranking and AHP method

Classes	Ranking method		AHP method		Absolute Difference	
	% area	km²	% area	km²	% area	km²
Very Low	2.92	7.20	11.16	27.53	8.24	20.33
Low	10.01	24.69	7.81	19.26	2.20	5.40
Low to Moderate	11.89	29.33	11.23	27.70	0.66	1.63
Moderate	12.93	31.88	16.75	41.31	3.82	9.45
Moderate to High	19.05	46.99	19.65	48.47	0.60	1.48
High	26.59	65.58	17.91	44.17	9.32	21.41
Very High	16.61	40.97	15.49	38.21	1.12	2.76

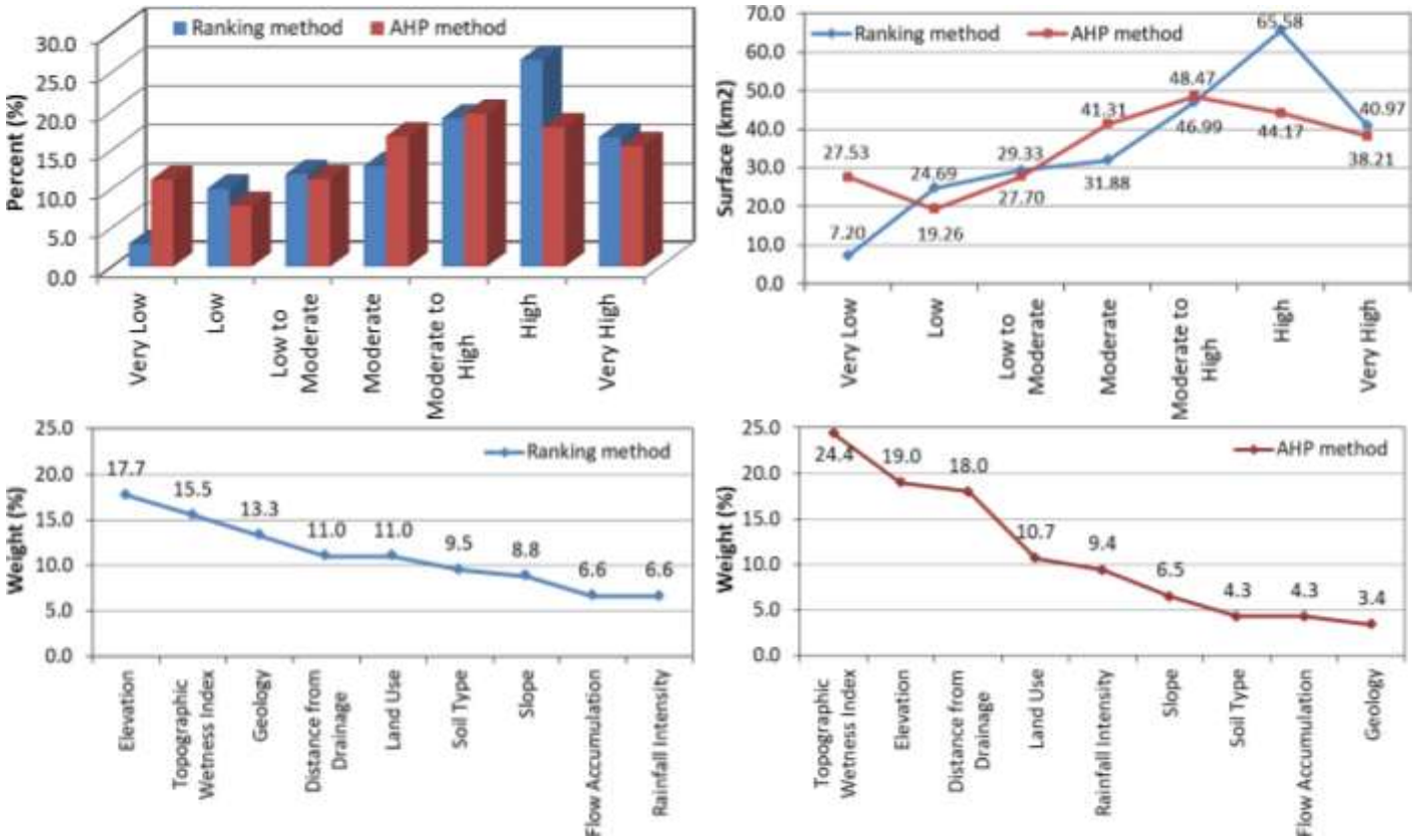

Chart -2: Graphical results' comparison between Ranking and AHP method

4. CONCLUSION

The purpose of the present study was to model the flood susceptible areas in a coastal, agricultural watershed, in Central Greece. The assessment of the flood prone areas is a key factor for a flood management strategy. An index-based methodology by means of weighted linear combination and multi-criteria analysis and evaluation method in a GIS environment was developed taking into account nine (9) parameters, namely, the flow accumulation (F), the rainfall intensity (I), the geology (G), the soil type (S_T), the land use (U), the basin's slope (S), the elevation (E), the distance from the drainage network (D) and the topographic wetness index (TWI). The relative weight of each parameter was calculated by two methods, the Ranking method and the Analytical Hierarchy Process using pairwise matrix comparison both combined by GIS techniques. Both methods considered that elevation, distance from drainage and TWI as well had the highest impact (weight) on flood occurrences, especially, within the flat relief (low slope gradient) at the East of the Atalanti river basin. The superimposition of each parameter resulted in mapping the area's flood susceptibility divided into seven (7) classes, from "Very Low" to "Very High". Red, orange and yellow colors on the map indicated a higher degree of vulnerability, increasing the flood risk. The resulting maps from both methodologies indicated that ~53-63% (~130-155 km^2) of the study area was subjected to "Moderate to High" up to "Very High" flood vulnerability due to the great extent of basin's flat relief (the lowland eastern part of the watershed with slopes under 2.0%). The tributaries and torrents were regarded as high flood prone areas and therefore by integrating the evaluation techniques with GIS, the decision and policy makers should take that in mind for effective planning tools and flood protection measures to reduce the flood risk and damage and to mitigate the flood consequences as well. These techniques were proved to be valuable and trustworthy for flood susceptibility assessment thanks to the capability of rapidly delineating the high risk potential areas with a very satisfactory degree of accuracy, however, they should be used as the initial flood analysis. Finally, the reliability of the application was confirmed by the historical flood records which were coincided with the high and very high flooding regions.

ACKNOWLEDGEMENT

The authors would like to express their thanks to the Hellenic Military Geographical Service (HMGS) for the topographical maps obtained as well as the Hellenic National Meteorological Service (HNMS) and the Ministry of Environment and Energy for the meteorological stations' precipitation dataset of the regional area.

CONFLICT OF INTERESTS

The authors confirm that there is no conflict of interests.

REFERENCES

[1] Bathrellos, G., Karymbalis, E., Skilodimou, H., Gaki-Papanastassiou, K., Baltas, E. 2016. Urban flood hazard assessment in the basin of Athens Metropolitan city, Greece. Environ. Earth Sci. 75, p.319.

[2] Chen, J., Hill, A., Urbano, L. 2009. A GIS-based model for urban flood inundation. Journal of Hydrology 373: pp.184–192.

[3] Chen, H., Ito, Y., Sawamukai, M., Tokunaga, T. 2015. Flood hazard assessment in the Kujukuri Plain of Chiba Prefecture, Japan, based on GIS and multicriteria decision analysis, Nat. Hazards, 78(1), pp.105–120.

[4] Kandilioti, G. and Makropoulos, C. 2012. Preliminary flood risk assessment. The case of Athens. Natural Hazards, 61 (2), pp.441–468.

[5] De Brito, M., Evers, M. 2016. Multi-criteria decision-making for flood risk management: a survey of the current state of the art, Nat. Hazards Earth Syst. Sci., 16(4), pp.1019–1033.

[6] De Brito, M., Evers, M., Delos, A., Almoradie, S. 2018. Participatory flood vulnerability assessment: a multi-criteria approach, Earth Syst. Sci, pp.373–390.

[7] Diakakis, M. 2017. Flood seasonality in Greece and its comparison to seasonal distribution of flooding in selected areas across southern Europe. J. Flood Risk Manag., 10, pp.30–41.

[8] Domakinis, C., Oikonomdis, D., Voudouris, K., Astaras, T., 2014. Using geographic information systems (GIS) and remote sensing to map flood extent and to assess flood hazard in Erythropotamos river basin (Evros, Greece), Proc. of 10th International Congress of the Hellenic Geographical Society, Thessaloniki.

[9] Emmanouloudis, D., Myronidis, D., Ioannou, K. 2008. Assessment of flood risk in Thasos Island with the combined use of multicriteria analysis AHP and geographical information system. Innov Appl Info Agric Environ, pp.103–115.

[10] Fernandez D., Lutz M. 2010. Urban flood hazard zoning in Tucuman Province, Argentina, using GIS and multicriteria decision analysis. Engineering Geology, 111, pp.90-98.

[11] Jeb, D., Aggarwal, S. 2008. Flood Inundation Hazard Modeling of the River Kaduna Using Remote Sensing and Geographic Information Systems, Journal of Applied Sciences Research, 4(12), pp.1822-1833.

[12] Karymbalis, E., Katsafados, P., Chalkias, C., Gaki-Papanastassiou, K. 2012. An integrated study for the evaluation of natural and anthropogenic causes of flooding in small catchments based on geomorphological and meteorological data and modeling techniques: The case of the Xerias torrent (Corinth, Greece). Zeitschrift für Geomorphologie 56 (1), pp.45-67.

[13] Kazakis, N., Kougias, I., Patsialis, T. 2015. Assessment of flood hazard areas at a regional scale using an index-based approach and Analytical Hierarchy Process: Application in Rhodope–Evros region, Greece, Science of the Total Environment 538, pp.555–563.

[14] Kourgialas, N., Karatzas, G. 2011. Flood management and a GIS modelling method to assess flood-hazard areas: a case study. Hydrol. Sci. J. 56 (2), pp.212–225.

[15] Kourgialas, N., Karatzas, G. 2017. A national scale flood hazard mapping methodology: The case of Greece–Protection and adaptation policy approaches. Science of the Total Environment, 601, pp.441-452.

[16] Lappas, I. 2018. Applied hydrogeological research in coastal aquifers. Case study of the coastal part of Atalanti region, Prefecture of Fthiotida. PhD Thesis Dissertation, School of Mining and Metallurgical Engineering, National and Technical University of Athens, p.487.

[17] Malczewski, J. 1999. GIS and Multiple-criteria Decision Analysis, New York: John Wiley & Sons.

[18] Maratos, G., Rigopoulos, K., Athanasiou, A. 1965. Geological maps of Atalanti and Livanates sheets, scale 1:50.000, Institute of Subsurface Geological Research.

[19] Meyer, V., Scheuer, S., Haase, D. 2009a. A multicriteria approach for flood risk mapping exemplified at the Mulde river, Germany, Nat. Hazards, 48(1), pp.17–39.

[20] Meyer, V., Haase, D. 2009b. A Multicriteria Flood Risk Assessment and Mapping Approach. Taylor & Francis Group, London.

[21] Myronidis, D., Emmanouloudis, D., Stathis, D., Stefanidis, P. 2009. Integrated flood hazard mapping in the framework of E.U directive on the assessment and management of flood risks. Fresenius Environ Bull, pp.102–111.

[22] Papaioannou, G., Vasiliades, L., Loukas, A. 2015. Multi-Criteria Analysis Framework for Potential Flood Prone Areas Mapping. Water Resource Management, pp.399–418.

[23] Patrikaki, O., Kazakis, N., Kougias, I., Patsialis, T., Theodossiou, N., Voudouris, K. 2018. Assessing Flood Hazard at River Basin Scale with an Index-Based Approach: The Case of Mouriki, Greece. Geosciences, 8, p.50.

[24] Pradhan, B. 2010. Flood susceptible mapping and risk area delineation using logistic regression, GIS and remote sensing. J Spat Hydrol 9(2).

[25] Saaty, T. 1977. A scaling method for priorities in hierarchical structures. Journal of Mathematical Psychology, 15 (3), pp.234-281.

[26] Saaty, T. 1980. The Analytic Hierarchy Process. McGraw-Hill, New York, pp.20-25.

[27] Saaty, T. 1990. How to Make a Decision: The Analytical Hierarchy Process, European Journal of Operational Research, 48, 1, pp.9-26.

[28] Sanders, R., Tabuchi, S. 2000. Decision support system for flood risk analysis for River Thames, United Kingdom, Photogrammetric Engineering and Remote Sensing, 66(10), pp.1185-1193.

[29] Stefanidis, S., Stathis, D. 2013. Assessment of Flood Hazard Based on Natural and Anthropogenic Factors Using Analytic Hierarchy Process (AHP), Natural Hazards, 68, 2, pp.569-585.

[30] Tsakiris, G. 2014. Flood risk assessment: concepts, modelling, applications. Natural Hazards Earth System Sciences 14: pp.1361-1369.

[31] Tsitroulis, I., Voudouris, K., Vasileiou, A., Mattas, C., Sapountzis, M., Maris, F. 2016. Flood hazard assessment and delimitation of the likely flood hazard zones of the upper part in Gallikos River Basin. In Procedings of the 14th International Conference, Thessaloniki, Greece, pp.995–1004.

[32] Yahaya, S., Ahmad, N., Abdalla, F. 2010. Multicriteria Analysis for flood vulnerable areas in Hadejia-Jama'are river basin, Nigeria. European Journal of Scientific Research, 42 (1), pp.71-83.

[33] Yalcin, G., Akyrek, Z. 2004a. Multiple criteria analysis for flood vulnerable areas. XXth ISPRS congress "geo-imagery briding continents", Turkey.

[34] Yalcin, G., Akyrek, Z. 2004b. Analyzing flood vulnerable areas with multicriteria evaluation, XXth International Society for Photogrammetry and Remote Sensing Congress.

[35] Youssef A., Pradhan B., Hassan A. 2011. Flash flood risk estimation along the St. Katherine road, southern Sinai, Egypt using GIS based morphometry and satellite imagery. Environmental Earth Sciences, 62(3), pp.611-623.